Baseline Validation of Unstructured Grid Reynolds-Averaged Navier-Stokes Toward Flow Control

R. D. Joslin and S. A. Viken

Baseline Validation of Unstructured Grid Reynolds-Averaged Navier–Stokes Toward Flow Control

Ronald D. Joslin*
Pennsylvania State University, State College, Pennsylvania 16804
and
Sally A. Viken[†]
NASA Langley Research Center, Hampton, Virginia 23681

I. Introduction

T HE value of the use of the Reynolds-averaged Navier–Stokes methodology for active flow control applications is assessed. An experimental flow control database exists for a NACA0015 airfoil modified at the leading edge to implement a fluidic actuator; hence, this configuration is used. Computational results are documented for the baseline wing configuration (no control) with the experimental results and assumes two-dimensional flow. The baseline wing configuration has discontinuities at the leading edge, trailing edge, and aft of midchord on the upper surface.

A limited number of active flow control applications have been tested in the laboratory and in flight. These applications include dynamic stall control using a deformable leading edge,[1] separation control for takeoff and landing flight conditions using piezoelectric devices,[2,3] pulsed vortex generators,[4] zero-net-mass oscillations,[5,6]

*Deputy Head, Applied Research Laboratory, Computational Modeling and Control Department, P.O. Box 30. Senior Member AIAA.

†Aerospace Engineer, Flow Physics and Modeling Department, Mail Stop 170.

and thrust vectoring with zero-net-mass piezoelectric-driven oscillatory actuation.[7]

As yet, there is no definitive comparison with experimental data that indicates current computational capabilities can quantitatively predict the large aerodynamic performance gains achieved with active flow control in the laboratory. However, one study[8] using the Reynolds-averaged Navier–Stokes (RANS) methodology has shown good quantitative agreement with experimental results for an isolated zero-net-mass actuator. In addition, some recent studies[9,10] have used RANS to demonstrate qualitative performance gains compared with the experimental data for separation control on an airfoil. Those quantitative comparisons for both baseline and flow control cases indicated that computational results were in poor quantitative agreement with the experiments.

The current research thrust will investigate the potential use of an unstructured grid RANS approach to predict aerodynamic performance for active flow control applications building on the early studies.[9,10] First the computational results must quantitatively match experiments for the no-control case before proceeding to the time-dependent flow control case. This paper documents the baseline (no-control) case using an unswept airfoil configuration.

The next section describes the configurations used for the computations and the experimentals. The computational approach is then described followed by results and concluding remarks.

II.   Airfoil Configurations and Experimental Data

Figure 1 shows the leading-edge and trailing-edge regions of the configurations used in the present study. The midchord regions for all airfoils are the same and, therefore, not shown in Fig. 1. A NACA0015 airfoil is used in the study to provide reference point results. The finite thick trailing edge of the NACA0015 airfoil matches
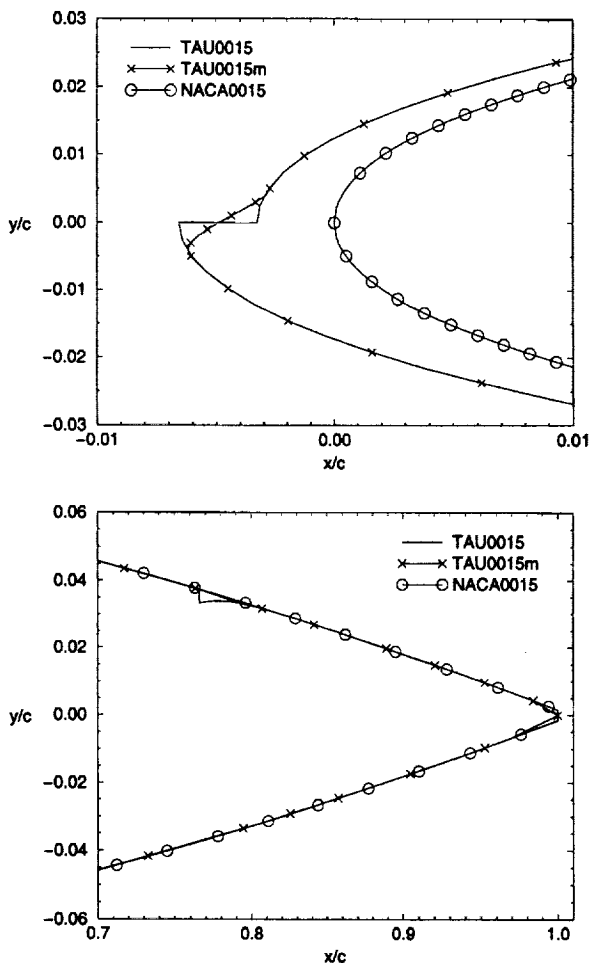
the TAU0015. The TAU0015 airfoil model was tested in a low-speed wind tunnel at the Tel Aviv University (TAU). The model is a NACA0015 airfoil modified in the leading-edge region to acommodate an actuation slot. Hence, the airfoil configuration is referred to as the TAU0015 airfoil. The TAU0015 model has a 0.3645-m chord, a 0.3% thick blunt trailing edge, and a 0.4% chord thick notch at 76.6% chord, which results from the flap/main element connection used in a different experiment. The actuator for the TAU0015 tests was located at the leading edge and leads to the 0.3% chord discontinuity (straight horizontal line region).

The previous computational studies[9,10] used single-block structured grid RANS and for convenience ignored the 76.6% chord notch and trailing-edge thickness and faired over (smoothed) the leading-edge discontinuity. Here, this altered configuration is referred to as TAU0015m; computational results from this model will be compared with the TAU0015 configuration. There is no experimental data for the numerically modified model.

The flow control experiments with the TAU0015 were conducted in the Meadow–Knapp Low Speed Wind Tunnel at the TAU.[5] The test section is 1.50 m high and 0.61 m wide. The TAU0015 model was instrumented with 36 static pressure taps, and measurements were made using a Scanivalve and a pressure transducer, 5 psi full scale. The transducer has an accuracy of 0.06% full scale. The freestream velocity of all tests was nominally 51 m/s. The pressure coefficient results are accurate to within ±0.6%. Lift, Cl, and drag, Cd, coefficients are obtained by integrating the measured pressures; accuracy in Cl is estimated to ±0.01 for prestall conditions and ±0.03 poststall. The drag coefficient Cd has experimental uncertainty of ±0.003 at prestall conditions and and ±10% at poststall conditions. The experimental conditions are at a Mach number of 0.15 and a chord Reynolds numbers of 1.2×10^6. The uncertainty in Reynolds number is ±2% due to variations in temperature and velocity during the tests.

The Cl and Cd for the experimental data are available at angle of attacks α from 0 to 24 deg in 2-deg increments. The maximum lift coefficient is $Cl = 1.056$ at $\alpha = 12$ deg and $Cd = 0.0288$. In addition, pressure coefficients Cp at $\alpha = 8$ and 22 deg are used for the current comparison.

III.   Computational Approach

The full unstructured Navier–Stokes two-dimensional RANS code (FUN2D)[11] will be used for the current study. The FUN2D code solves the time-dependent RANS equations expressed as a system of conservation laws relating the rate of change of mass, momentum, and energy in a control volume to the fluxes of these quantities through the control volume. The solver is an implicit, upwind-differencing algorithm with the inviscid fluxes obtained on each face of the control volume with Roe's flux-difference-splitting scheme. The node-based algorithm stores the variables at the vertices of the mesh, and the equations are solved on the nonoverlapping control volumes surrounding each node. The viscous terms use a central difference formulation evaluated with the finite volume formulation. Time advancement is made with a linearized first-order backward Euler scheme. At each time step, the equations are solved with 15 Gauss–Seidel subiteratives, sequentially solving for all odd numbered nodes and then all even numbered nodes. A two-level V-type multigrid approach is used for this baseline study to accelerate convergence.[12] A very fine grid was first used to determine the effect of the geometric discontinuities on the aerodynamic performance. Then grid coarsening was implemented to minimize the grid requirements for accurate results and more efficient computations. The Spalart–Allmaras (SA) turbulence model[13] is used in this investigation, and all computations involve fully turbulent flow. A computer workstation is used for the present study.

The unstructured grids were generated with advancing-front-type point placement with iterative local remeshing for grid quality improvement.[14,15] Figure 2 shows an initial coarse grid around the TAU0015 airfoil, resolving all discontinuities on the configuration. Similar grids were generated for the TAU0015m and NACA0015 airfoils. The grids extend from the airfoils to form a far-field circle with a radius of 20 chord lengths around the airfoils.

Fig. 1   NACA0015, TAU0015, and TAU0015m airfoils.

Table 1   Number of nodes used for initial computations

Configuration	Grid1 total	Grid1 surface	Grid2 total	Grid2 surface
TAU0015	114,119	1,891	51,150	1,260
TAU0015m	48,063	1,032	21,316	516
NACA0015	62,764	1,100	25,352	550
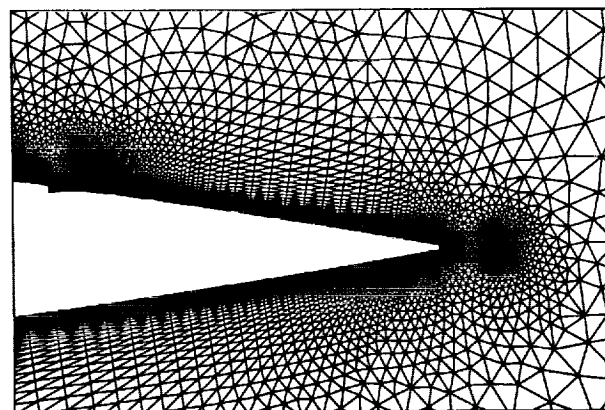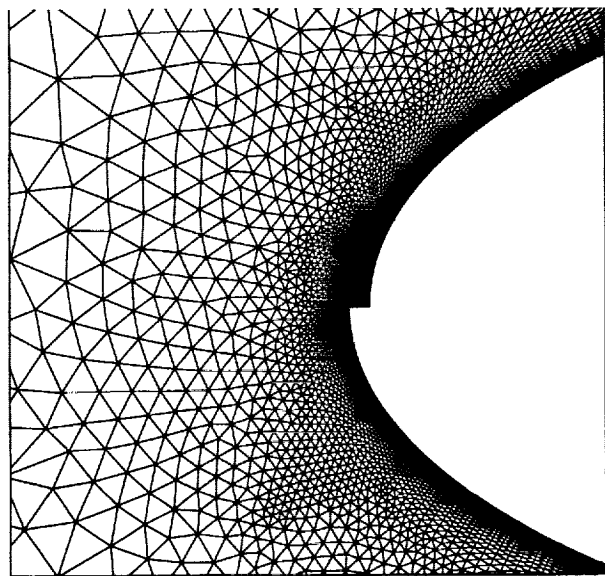
Fig. 2   Coarse grid for TAU0015 airfoil.
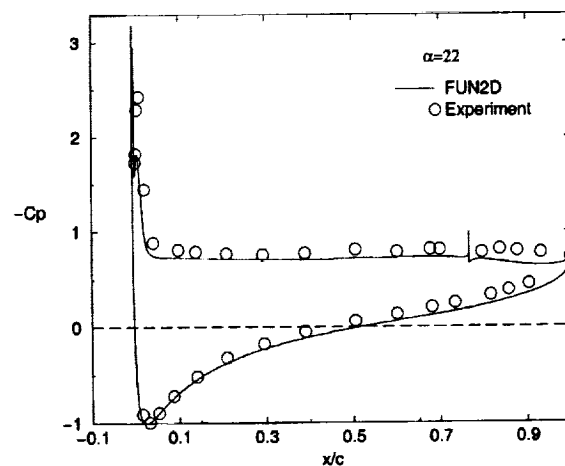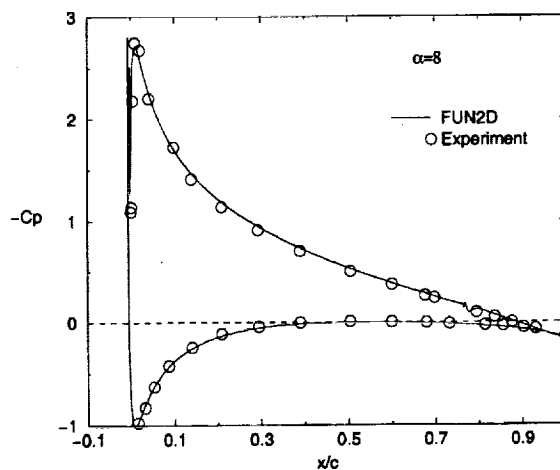
IV.   Results

All grids in the initial computations had the first near-surface grid point below $y^+ = 0.7$ to ensure the sublayer of the turbulent shear flow was sufficiently resolved. This specification of the first grid point approximation is based on relationships between y^+, Reynolds number, and skin friction for a flat plate boundary layer. For turbulent flow, this relationship yields an analytical relationship between y^+ and the first wall-normal grid point. This relationship is $y^+ = \Delta y \cdot \sqrt{(c_f/2)Re}$, where $c_f \simeq 0.455/\ell_n^2(0.06Re_x)$ and Δy is the physical distance for the first grid point away from the airfoil surface. Specifying a midchord $y^+ = 0.102$ will keep all near-wall points below 0.7, as will be shown later.

The number of surface nodes and total grid nodes for the first comparison are shown in Table 1 for each airfoil. The TAU0015 airfoil grid has significantly more grid points because of the grid clustering near the surface discontinuities, which are not present in the TAU0015m and NACA0015 airfoils.

Convergence of the steady-flow computations was achieved when the change in Cl was less than 0.015% per iteration. At this criterion, Cd was changing by less than 0.005% per iteration. The only

unsteadiness in the computations was observed at $\alpha = 26$ deg; unsteady vortex shedding was evident.

Figure 3 shows the computed Cl with variation in α for the NACA0015, TAU0015, and TAU0015m airfoils compared with the experimental data. For the NACA0015, the maximum Cl and stall α are 30% and 4 deg higher than the experimental data. For the TAU0015m airfoil, the maximum Cl and stall angle are 23% and 2 deg higher than the experiments. These overpredictions for the TAU0015m airfoil are consistent with the earlier studies,[9,10] which used the same airfoil but a structured grid and two different RANS
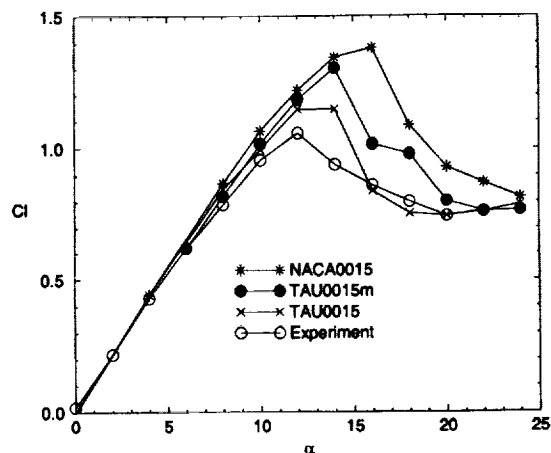
Fig. 3   Computed Cl vs α for TAU0015, TAU0015m, and NACA0015 airfoils compared with experimental data.

Fig. 4   Computational and experimental pressure coefficients Cp for TAU0015 airfoil at $\alpha = 8$ deg (prestall) and 22 deg (poststall).

codes. In closer agreement, the computed results for the TAU0015 airfoil approach the experimental results, overestimating the stall angle by 2 deg and the maximum Cl by 9%. Thus, the subtle differences in geometry for the NACA0015, TAU0015m, and TAU0015 airfoils have led to large differences in the computed stall α and maximum Cl.

A reasonable explanation for the differences between computational and experimental results for the TAU0015 geometry may be obtained with a careful review of the experimental results. In the experiments, Cl and Cd are derived from numerical integration of the static pressure measurements. Hence, a comparison of computed and measured pressure information is necessary for this review. Figure 4 shows computed pressure coefficients Cp for the TAU0015 airfoil compared with experimental results for $\alpha = 8$ deg (prestall) and 22 deg (poststall). The computational results show pressure spikes at the leading edge and near 76% chord resulting from the geometrical discontinuities. No pressure spikes were measured in the wind-tunnel experiments because no taps were or could be positioned on the actuator. Therefore, the experiments could not capture the additional pressure spike predicted in the computations. Based on this understanding of the experimental data, the computed Cl and Cd are now obtained by integrating the pressure over the TAU0015 airfoil in regions consistent with the experimental pressure taps. Only the contribution from the leading-edge actuator discontinuity are excluded in this new Cl and Cd. The Cl and Cd vs α are compared with experimental data in Fig. 5. The computed maximum Cl is now overpredicted by 2% compared with the experimental data, and the stall α are in agreement at 12 deg. The overprediction in lift results in an underprediction of the drag. The poststall (separated) conditions show notable disagreement between computational and experimental results. Whereas the SA turbulence model has not been developed or validated for separated flows, significant uncertainty

exists in experimental error assessment for separated flow regions. Unless the 36 pressure taps used in the experiments were positioned to capture all of the essential physics of the separated flow, large (unpredictable) uncertainty could exist for the Cl and Cd values. Such experimental uncertainty for poststall conditions is confirmed in results for a simple NACA0012 airfoil.[16,17] Hence, the computational and experimental results have uncertainty in their respective quantities for highly separated flow conditions.

In any grid generation process, some judgment must be made concerning the adequacy of the grids for the computations. This is usually facilitated by grid refinement studies. Such a study was carried out but is not reported due to space limitations. The grid refinement analysis confirms the validity of the reported grids.

V. Conclusions

Results from an unstructured-grid RANS code were used to analyze the possible impact of small geometric differences in airfoils on aerodynamic performance. Results for NACA0015, TAU0015, and TAU0015m airfoils were compared with experimental data for the TAU0015 airfoil configuration. The TAU0015 airfoil has discontinuities at the leading edge, trailing edge, and aft of midchord on the upper surface.

The TAU0015m was similar to the TAU0015 except the leading-edge shape was smoothed to make the geometry more continuous and the midchord notch was ignored. The current TAU0015m results are in agreement with previous investigations.

A comparison of the results from the various airfoils suggests that the midchord discontinuity does not affect the aerodynamics of the wing and can be ignored for more efficient computations. The leading-edge discontinuity significantly affects the lift and drag; hence, the integrity of the leading-edge notch discontinuity must be maintained in the computations to achieve a good match with the experimental data.

The analysis of computed performance vs experimental data for the TAU0015 airfoil demonstrated that consistency in determining lift and drag coefficient quantities was important to achieve quantitative agreement. The integration of computed pressure should be contained to regions of the airfoil consistent with the pressure taps.

Future activities for the validation of RANS for active flow control will include an investigation of the accuracy of RANS for time-dependent flow problems, the introduction of boundary conditions to model the oscillatory actuation, and an evaluation of oscillatory excitation on the aerodynamic performance. The oscillatory excitation results will be compared with experiments for the current TAU0015 configuration.

Acknowledgments

References

[1]Chandrasekhara, M. S., Wilder, M. C., and Carr, L. W., "Control of Flow Separation Using Adaptive Airfoils," AIAA Paper 97-0655, Jan. 1997.

[2]Seifert, A., Bachar, T., Wygnanski, I., Kariv, A., Cohen, H., and Yoeli, R., "Application of Active Separation Control to a Small Unmanned Air Vehicle," Journal of Aircraft, Vol. 36, No. 2, 1998, pp. 474–477.

[3]Seifert, A., Eliahu, S., Greenblatt, D., and Wygnanski, I., "Use of Piezoelectric Actuators for Airfoil Separation Control," AIAA Journal, Vol. 36, No. 8, 1998, pp. 1535–1537.

[4]McManus, K., and Magill, J., "Separation Control in Incompressible and Compressible Flows Using Pulsed Jets," AIAA Paper 96-1948, June 1996.

[5]Seifert, A., Darabi, A., and Wygnanski, I., "Delay of Airfoil Stall by Periodic Excitation," Journal of Aircraft, Vol. 33, No. 4, 1996, pp. 691–698.

[6]Seifert, A., and Pack, L. G., "Oscillatory Excitation of Unsteady Compressible Flows over Airfoils at Flight Reynolds Numbers," AIAA Paper 99-0925, Jan. 1999.

[7]Pack, L. G., and Seifert, A., "Periodic Excitation for Jet Vectoring and Enhanced Spreading," AIAA Paper 99-0672, Jan. 1999.

[8]Kral, L. D., Donovan, J. F., Cain, A. B., and Cary, A. W., "Numerical Simulation of Synthetic Jet Actuators," AIAA Paper 97-1824, June 1997.

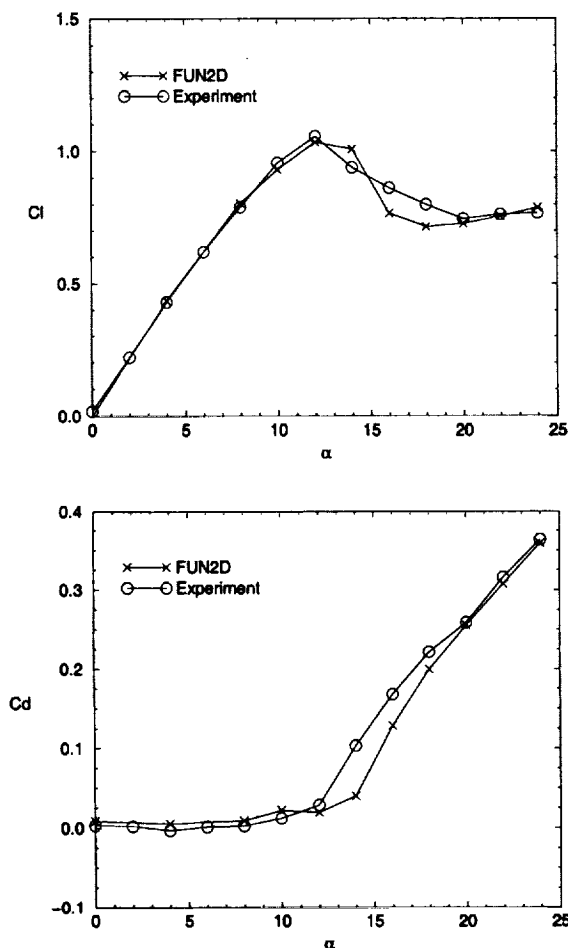[9]Donovan, J. F., Kral, J. D., and Cary, A. W., "Active Flow Control Applied

Fig. 5 Computed Cl and Cd vs α compared with experimental data for TAU0015 airfoil.

to an Airfoil," AIAA Paper 98-0210, Jan. 1998.

[10]Ravindran, S. S., "Active Control of Flow Separation over an Airfoil," NASA/TM-1999-209838, Dec. 1999.

[11]Anderson, W. K., and Bonhaus, D. L., "An Implicit Upwind Algorithm for Computing Turbulent Flows on Unstructured Grids," *Computers and Fluids*, Vol. 23, No. 1, 1994, pp. 1-21.

[12]Anderson, W. K., Rausch, R. D., and Bonhaus, D. L., "Implicit/ Multigrid Algorithms for Incompressible Turbulent Flows on Unstructured Grids," *Journal of Computational Physics*, Vol. 128, 1996, pp. 391-408.

[13]Spalart, P. R., and Allmaras, S. R., "A One-Equation Turbulence Model for Aerodynamic Flows," AIAA Paper 92-0439, Jan. 1992.

[14]Marcum, D. L., "Generation of Unstructured Grids for Viscous Flow Applications," AIAA Paper 95-0212, Jan. 1995.

[15]Marcum, D. L., and Weatherhill, N. P., "Unstructured Grid Generation Using Iterative Point Insertion and Local Reconnection," *AIAA Journal*, Vol. 33, No. 9, 1995, pp. 1619-1625.

[16]McCroskey, W. J., McAlister, K. W., Carr, L. W., and Pucci, S. L., "An Experimental Study of Dynamic Stall on Advanced Airfoil Sections Volume 1. Summary of the Experiment," NASA TM 84245, July 1982.

[17]McCroskey, W. J., "A Critical Assessment of Wind Tunnel Results for the NACA 0012 Airfoil," CP-429, AGARD, 1987.